Molecular Dynamics Simulation of Converting Waste Polyethylene (PE) to Chemicals and Fuels under Non-Isothermal and Isothermal Conditions

Zhiheng Xu [1], Qiyuan Xie [1*], Cheng Chen [2], Xi Jiang [2*]

[1] State Key Laboratory of Fire Science, University of Science and Technology of China, Hefei, 230027, China

[2] School of Engineering and Materials Science, Queen Mary University of London, Mile End Road, London E1 4NS, UK

*Corresponding authors. Email: xqy@ustc.edu.cn; xi.jiang@qmul.ac.uk

Highlights

- Post pyrolysis is characterized by the decreasing of gaseous pyrolysis products.
- Heating rates play an important role in the carbon number distribution of products.
- Temperature range for optimal recovery of C_2H_4 and C_3H_6 is identified.
- Re-aggregation of gas into oil results in reduced generation of gas at high temperatures.
- The effect of reaction time depends on the pyrolysis temperature.
- Detailed pathways are identified and analyzed for reactions of C_2H_4 and C_3H_6.

ABSTRACT

Pyrolysis, one method of chemical recycling, has been an effective and clean way for processing plastic solid waste (PSW), which is a heavy burden for sustainable development. Series of molecular dynamic simulations are carried out for detailed pyrolysis of polyethylene (PE) waste using reactive force field (ReaxFF) for both non-isothermal and isothermal conditions. The results show that the PE pyrolysis at non-isothermal conditions can be divided into four stages. The last stage (post pyrolysis) is analyzed in depth, which shows decreasing of short-chain products and increasing of relatively long-chain components at high temperatures. Pyrolysis of PE at high heating rates reduces oil cracking and results in high yield of oil. The effect of reaction time depends on the pyrolysis temperature. In addition, under isothermal pyrolysis conditions, the simulated temperature range of 2500-2750 K is optimal for more recovery of C_2H_4 and C_3H_6 due to its high yield and mild influence of reaction time. Finally, detailed mechanisms of generation and consumption of C_2H_4 and C_3H_6 of PE pyrolysis are demonstrated. The regeneration of long-chain oil in the late stage of PE pyrolysis and the corresponding mechanisms are illustrated. The results in this study can be used to guide the design of systems for PSW processing with recovery of chemicals and fuels.

Keywords: Molecular dynamic simulation; Polyethylene waste; ReaxFF; Pyrolysis; Reaction mechanisms.

1. Introduction

More and more plastic solid wastes (PSWs) are a heavy burden for sustainable development and environmental protection, although plastics used to be one of the greatest inventions [1]. It has been fully recognized that landfill or incineration of PSW is not an environmentally friendly way for plastic waste disposal because of the extremely slow degradation of the underground PSW or the generation of hazardous burning products [2-4]. On the other hand, chemical recycling using pyrolysis or gasification provides an effective, clean and economic way for PSW processing, which gets more and more attention [5-7]. In recent years, the conversion of PSW into valuable fuels and chemicals by pyrolysis has been considered as a promising approach to processing PSWs [8, 9]. Pyrolysis is the thermochemical decomposition of the waste materials in the absence of oxygen, leading to the formation of gases, liquids, and solid residuals that can be used as chemicals and fuels.

Waxes, light olefins and oils are the main products currently expected to be obtained by PE pyrolysis. Many researchers focused on the evaluation of the influence parameters such as the pyrolysis reactors [10, 11], temperature [12-14], residence time [14, 15], and catalysts [16, 17] on improving the selectivity of the target products. Elordi et al. [18] carried out continuous pyrolysis of high-density polyethylene (HDPE) in a conical spouted bed reactor and found that the optimum temperature for wax production was a relatively low temperature of 500°C with a wax yield of 70%. Some previous works have shown that relatively low temperature and short residence time are conducive to producing high yields of oil [13, 19]. Hernandez et al. [20] used fluidized bed reactor for PE pyrolysis from 400 to 800°C, and found that the yields of the main gas fractions ethylene (C_2H_4) and propylene (C_3H_6) both increased with increasing pyrolysis temperature and reached a maximum yield of 16.5% and 10.5% respectively at 800°C. Similar results were obtained by Conesa et al. [21], who also found that the yield of C_2H_4 and C_3H_6 decreases significantly if the temperatures were higher than 800 °C. Mastral et al. [14] identified a significant effect of residence time on PE pyrolysis. When the residence time varied from 0.99 to 1.46 s at 650 °C, the C_2H_4 yield increased from 2.6% to 7.5%. Meanwhile, when the temperature reached 850 °C, C_2H_4 yield began to decrease with increasing residence time (>0.86 s). Therefore, it is considered that high temperature (>700 °C) and short residence time are highly advantageous for more recovery of light olefins. However, the combined effects and the relationships of various parameters of the pyrolysis process (such as the dependence of residence time on pyrolysis temperature) have not been fully understood. In addition, very limited analyses were reported for the overall pyrolysis stages, the corresponding distributions of fuel products and the reaction mechanisms involved at each stage. The detailed information about

the formation and further consumption of olefin monomers, the role of radicals, and the influence of heating conditions are still not clear for optimal design of plastics pyrolysis in engineering applications.

Recently, molecular simulations have been used in pyrolysis due to their ability to observe the details of chemical reactions directly at the atomic level, which is beyond the capabilities of experimental measurements. Quantum mechanics / chemistry are powerful tools for understanding chemical reactions, but the high computing cost prohibits their broader application to the pyrolysis of polymer systems [22]. Classical molecular dynamics (MD) simulation can be used to study models with more than tens of thousands of atoms. However, classical MD cannot be used to obtain information on chemical bond breakage and formation [23]. Reactive force field molecular dynamics (ReaxFF MD), which was developed by van Duin et al. [24], has been increasingly used because of the precise depiction of the particulars in chemical reactions. It is worth noting that, conditions used in MD simulations are often not the same as those in laboratory experiments. It is a common strategy to use relatively higher temperature in ReaxFF MD simulation to increase the collision rate, thereby making reactions occur at picosecond scale [25]. Nevertheless, there may be a correspondence between the experimental and computational values used in MD simulation. It has been validated extensively that pyrolysis kinetics and products distribution of ReaxFF MD simulation correlate well with experimental results for a wide range of chemical substances such as polyvinyl chloride, coal, PE, cellulose and lignin [26-29]. Based on ReaxFF MD simulations, Liu et al. [30] discovered that the major reactions of high-density polyethylene (HDPE) pyrolysis process included homolysis, β-scission, radical addition and H-abstraction etc. were observed. Wang et al. [31] investigated the co-pyrolysis process and mechanism of cellulose and PE using ReaxFF MD simulations. It was found that co-pyrolysis facilitated the generation of alcohols and hydrocarbon products, and the presence of PE significantly enhanced the quality of the products. Hong et al. [26] explored the co-pyrolysis of Zhundong coal with polyethylene (PE) and polystyrene (PS) using ReaxFF. The results showed that coal promoted the pyrolysis of PE at low temperatures but had little effect at high temperatures, while PE had an opposite effect on the pyrolysis of coal. The previous studies provided insightful information on pyrolysis mechanism of plastics at high temperatures, which also indicated the efficacy of using ReaxFF MD for simulating pyrolysis of different materials such as plastics, biomass and coal. In general, previous studies have demonstrated that the reaction paths and intermediate processes of PE pyrolysis can be revealed by using ReaxFF MD.

In this study, aiming at improving the selectivity for the target products (oil and light olefins), series of ReaxFF MD simulation were carried out to investigate the detailed pyrolysis of PE under

both isothermal and non-isothermal conditions. Based on ReaxFF MD simulations, the thermal cracking behaviours of PE at different heating stages and the corresponding products distribution were analysed. The reaction mechanism leading to a decrease in the yield of light olefins (C_2H_4 and C_3H_6) at high temperatures was also investigated.

2. Method of ReaxFF MD

2.1. Molecular model of PE

The first step of the ReaxFF MD simulation is the construction of a suitable molecular structure model for characterizing the PE material. The degree of polymerization, which represents the molecular weight of polymer molecule, plays an important role in MD simulation of PE pyrolysis. Here, each PE molecule ($C_{120}H_{242}$) is designed as a polymerization by 60 monomers after considering the representation of PE molecular characteristics, pyrolysis complexity and computational cost. A previous study [26] suggested that this polymerization degree is sufficient for the pyrolysis analyses of PE and other polymers through ReaxFF MD simulation.

Specifically, a pyrolysis system consisting of 10 PE chains was built in a computational box with periodic boundaries. To eliminate overlapping of atoms, the original density of the PE system was set as 0.6 g/cm^3. Then, five annealing cycles from 300 to 1000 K were performed in the constant-temperature, constant-volume (NVT) ensemble for geometric optimization of the system. Subsequently, to achieve the desired PE density of 0.8 g/cm^3, the isothermal–isobaric (NPT) ensemble was used to modify the molecular system for 200 ps at 0.1 MPa and 300 K. Finally, the energy minimization of the model was performed. In this way, as shown in Fig. 1, an optimized PE molecular system with 3620 atoms and a density of 0.8 g/cm^3 was finally constructed. It should be noted that the density of PE molecular system obtained in the ReaxFF MD simulations cannot be exactly the same as but as close as possible to the actual one based on the geometric optimization of the NVT and NPT ensembles. The system density is consistent with that of the PE molecular system in recent studies [26, 31].
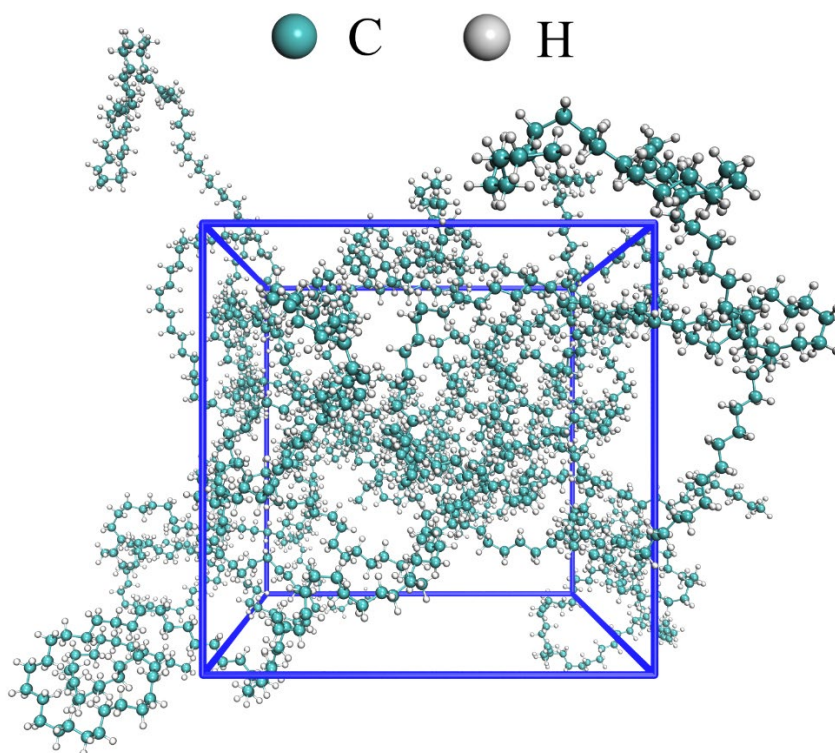
Fig. 1. PE molecular system with 10 chains (*n*=60) in the computational box.

2.2. Cases for PE pyrolysis

Based on the constructed PE molecular system, the pyrolysis behavior can be simulated in the NVT ensemble at various heating conditions. Here two series of ReaxFF MD simulation were carried out for PE pyrolysis at non-isothermal and isothermal heating conditions. For the non-isothermal cases, after a series of pre-simulations, three viable heating rates (2, 10 and 20 K/ps) were chosen to analyze the impact of heating rate on PE pyrolysis and to investigate the pyrolysis mechanisms in detail. The case of 2 K/ps represents the PE pyrolysis at a low heating rate while the other two cases represent the cases at higher heating rates. Additionally, the temperature of simulations increased from 300 to 3000 K. For the isothermal pyrolysis cases, the constant temperatures were set as 2000, 2250, 2500, 2750, 3000, 3500 and 4000 K respectively with the pyrolysis time of 250 ps. In this way, the effects of the heating rate, temperature and the corresponding reaction time (similar to the residence time in the experiment) on the pyrolysis evolution can be analyzed through comparison. The high temperature setting in ReaxFF simulations was used to speed up the reaction kinetics and to compress the reaction time scale [32]. Furthermore, the simulation results in previous work achieved at high temperatures are very close to the experimental data [29, 33, 34].

All the MD simulations here are conducted in the Large-scale Atomic/Molecular Massively Parallel Simulator (LAMMPS) [35] using the ReaxFF reactive force field for hydrocarbon [36]. Periodic boundary conditions were imposed in all directions of the cubic box with the edge length of 32.7 Å. The Nose-Hoover thermostat with a damping constant of 100 fs was used to govern the simulation temperature. The atom movements were updated with a time step of 0.25 fs for all simulations. Finally, a bond order cutoff distance of 0.3 Å was used to identify the product components.

3. Results and discussion

3.1. Non-isothermal pyrolysis of PE

In this study, the first step was to establish a mapping between the conditions used in MD simulation and (TG) experiment of pyrolysis. The data of the non-isothermal simulations was obtained from three independent pyrolysis simulations at 2 K/ps. It was shown that the difference between the results of repeated cases was very small, which suggested the reliability of ReaxFF MD simulations for PE pyrolysis. Drawing on the approach in previous research, the mass loss characteristics of non-isothermal simulations are compared with our TG experimental results as illustrated in Fig. 2(a). As shown in Fig. 2(b), the activation energy for PE pyrolysis is estimated to be 383.65 kJ/mol (ReaxFF MD) and 390.87 kJ/mol (TG experiment) according to the first order reaction model [26, 29], which can be expressed in the following equation

$$\ln\left[\frac{-\ln(1-\alpha)}{T^2}\right] = \ln\left(\frac{AR}{\beta E_a}\right) - \frac{E_a}{RT} \tag{1}$$

where α is the conversion, T represents the temperature, A is the pre-exponential factor, R represents the universal gas constant, and β denotes the heating rate. In Fig. 2(b), the activation energy (E_a) was calculated by plotting $\ln[-\ln(1-\alpha)/T^2]$ versus $1/T$. It can be seen from Fig. 2 that the experimental temperature range of 650 to 825K with heating rate of 2 K/min corresponds to a MD simulated temperature range of 1750 to 3000K with heating rate of 2 K/ps, while the activation energy values are very close to each other. The closeness of the activation energies between the simulations and experiments is due to the calculation method of the activation energy using the slope of the graph. For the mass loss curves, their similarity is mainly the result of the corresponding mapping between the thermal pyrolysis in molecular systems and that in the microscale level.
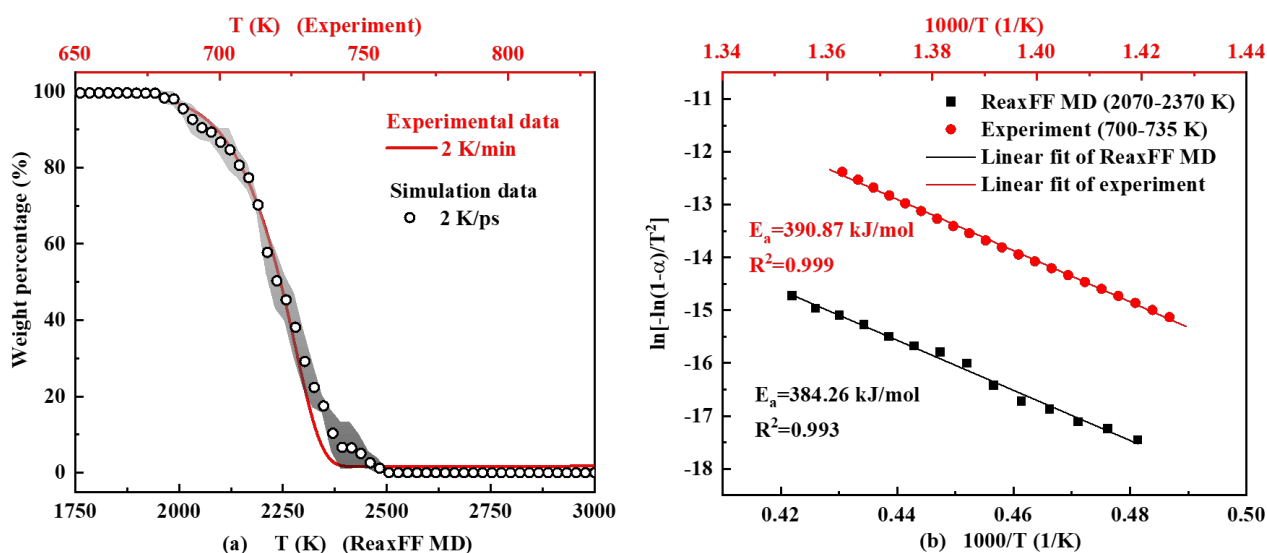
Fig. 2. Comparison of ReaxFF MD simulation and TG experiment results: (a) Mass loss of PE pyrolysis; (b) Plots of $\ln[-\ln(1-\alpha)/T^2]$ versus $1/T$ of main mass loss stage of PE.

Based on the mapping information shown in Fig. 2, non-isothermal pyrolysis MD simulations were carried out to investigate the effect of heating rates on PE pyrolysis. Normally, the products of PE thermal cracking are divided into gas (C_0-C_4), oil (C_5-C_{20}) and wax ($>C_{20}$), respectively [18, 37]. Fig. 3 presents the evolution of gas, oil and wax during PE pyrolysis in 300-3000 K at the heating rates of 2, 10 and 20 K/ps, respectively. The stages of the PE pyrolysis process are divided based upon the continuous observation of the product evolution and molecule trajectories. As shown by the regions with different colors in Fig. 3(a), at the heating rate of 2 K/ps, the PE pyrolysis evolution can be mainly divided into four stages: structure adjustment and activation, initial pyrolysis, deep degradation and post pyrolysis. The first stage (Stage 1) is mainly in the temperature range of 300-1988 K. A few long chains break and small molecules (such as C_2H_4 and some radicals) are generated in this stage. The main molecular behaviors are the configuration adjustment and activation of PE long-chain structures. At temperatures of 1988-2460 K in Stage 2, more and more oil and gas components are generated with the consumption of wax fractions as the temperature further increases. At the end of Stage 2, the oil yield basically reaches a stable value. In Stage 3 with temperatures in 2460-2730 K, many gas components are rapidly produced through the degradation of oil and waxes. The weight percentage increase of gas is almost 50%. Therefore, the division boundary between initial pyrolysis (Stage 2) and deep degradation (Stage 3) is the transition of the generation into consumption for the oil group. This specific temperature point is supposed to be important for the fuel recovery of plastics in practical applications.

For the last pyrolysis stage (Stage 4) in the temperature range of 2730-3000 K, wax is completely pyrolyzed into oil and gas. The weight percentages of the oil and gas are relatively steady with

percentages of about 10% and 90% throughout this stage despite the further increasing of temperature. However, at the end of this stage, it seems that some gas products are transformed into oil products. The unexpected results suggest that the enhanced activity of monomer molecules at such high temperatures might result in addition reactions between the short-chain gas components and radicals in the stage of post pyrolysis at high temperatures.

As shown in Figs. 3(b) and (c), for the heating rates of 10 and 20 K/ps, many characteristics during the pyrolysis evolution, such as the decrease of wax, the increases of oil and gas with the increasing of temperature, are similar to those in Fig. 3(a). There are also some differences for the PE pyrolysis results among varied heating rates. Firstly, the critical temperatures for the adjacent stages shift towards high temperatures, which are mainly induced by the thermal hysteresis. In this way, there are only three pyrolysis stages (no post pyrolysis stage) for the heating rates of 10 and 20 K/ps in the temperature range of 300-3000 K. Secondly, as shown in Fig. 3(d), the peaks for oil products are higher for the non-isothermal pyrolysis cases with higher heating rates at relatively higher temperatures, which are 26.7%, 24% and 32.5% at 2460 K, 2865 K and 2865 K, respectively. Finally, for the pyrolysis in Stage 2, as shown in Fig. 3(b) and (c), the yields of the oil are higher than gas for heating rates of 10 K/ps and 20 K/ps, which is different in Fig. 3(a). Further analyses of the detailed pyrolysis of PE at different heating rates are presented subsequently.
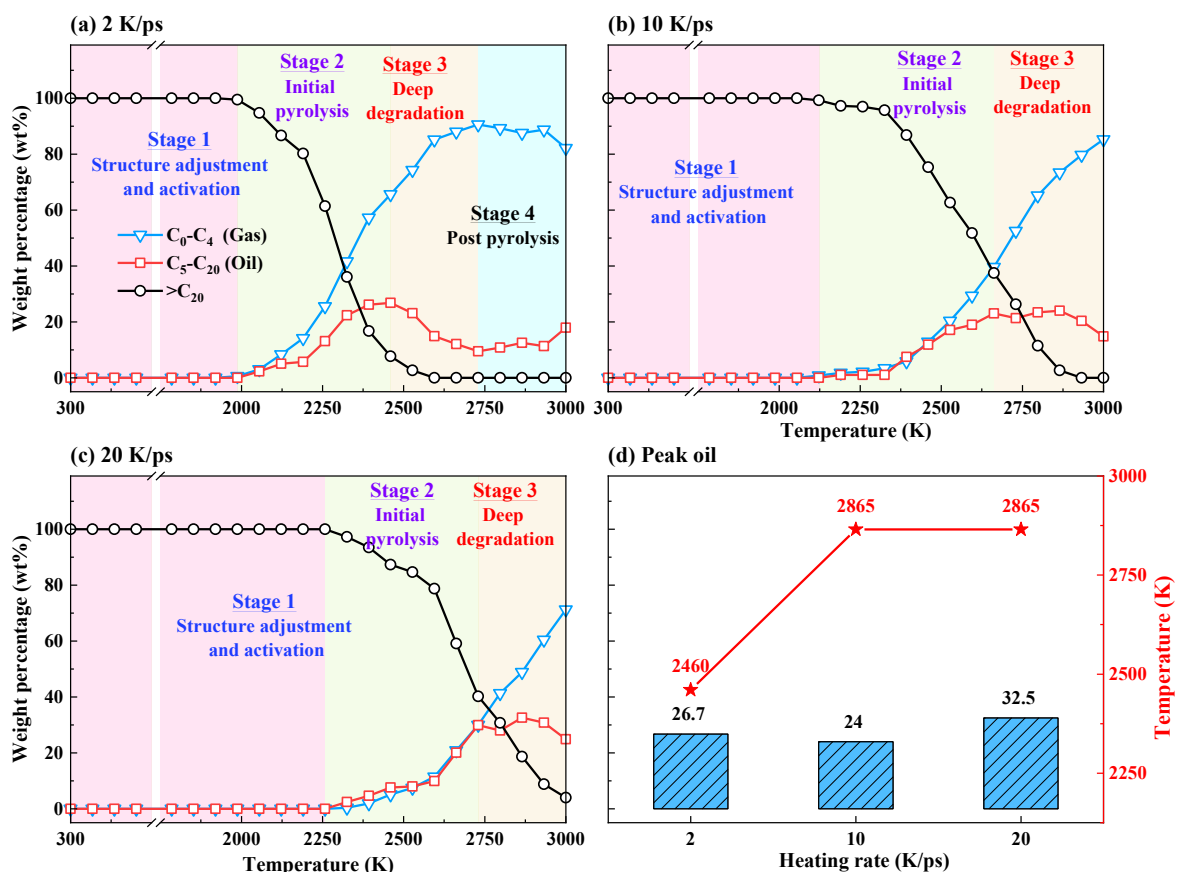
Fig. 3. Evolution of product groups (wax, oil, gas) for PE pyrolysis in 300-3000 K at different heating rates: (a) 2 K/ps; (b) 10 K/ps; (c) 20 K/ps; (d) Peak of oil and the corresponding temperatures.

In order to gain more details of the PE pyrolysis mechanism at varied heating rates, Fig. 4 shows the distribution of products with various carbon numbers (C_5-C_{40}) at typical temperatures (2000, 2250, 2500, 2750 and 3000 K). As shown in Fig. 4(a), in the case of 2 K/ps, the result suggests that more short-chain components are generated. At the temperature of 2500 K, there are hardly any C_{20+} compounds. In addition, most of the oil products are C_5-C_{10} fractions as the temperature increases to 2750 K. However, more products with longer chains (C_5-C_{15}) are generated during the temperature increase from 2750 to 3000 K, which is also illustrated by the specific increase of oil products at the same temperature range in Fig. 3(a). For the case of 10 K/ps, as shown in Fig. 4(b), at the temperatures of 2500 and 2750 K, comparing with those in Fig. 4(a), the distribution of oil products with different carbon numbers is relatively uniform. The uniform distribution of C_5-C_{40} products against carbon numbers is more obvious when the heating rate is further increased to 20 K/ps, as shown in Fig. 4(c). Therefore, the combined results in Figs. 3 and 4 indicate that not only the production rates of oil and gas, but also the detailed composition of the products are strongly affected by the heating rates during the PE non-isothermal pyrolysis. A higher heating rate promotes the production of more oil with a

uniform carbon number distribution. The results here also indicate the necessity for MD simulation in isothermal conditions to investigate the pyrolysis mechanism of PE at typical high temperatures for a sufficiently long time.
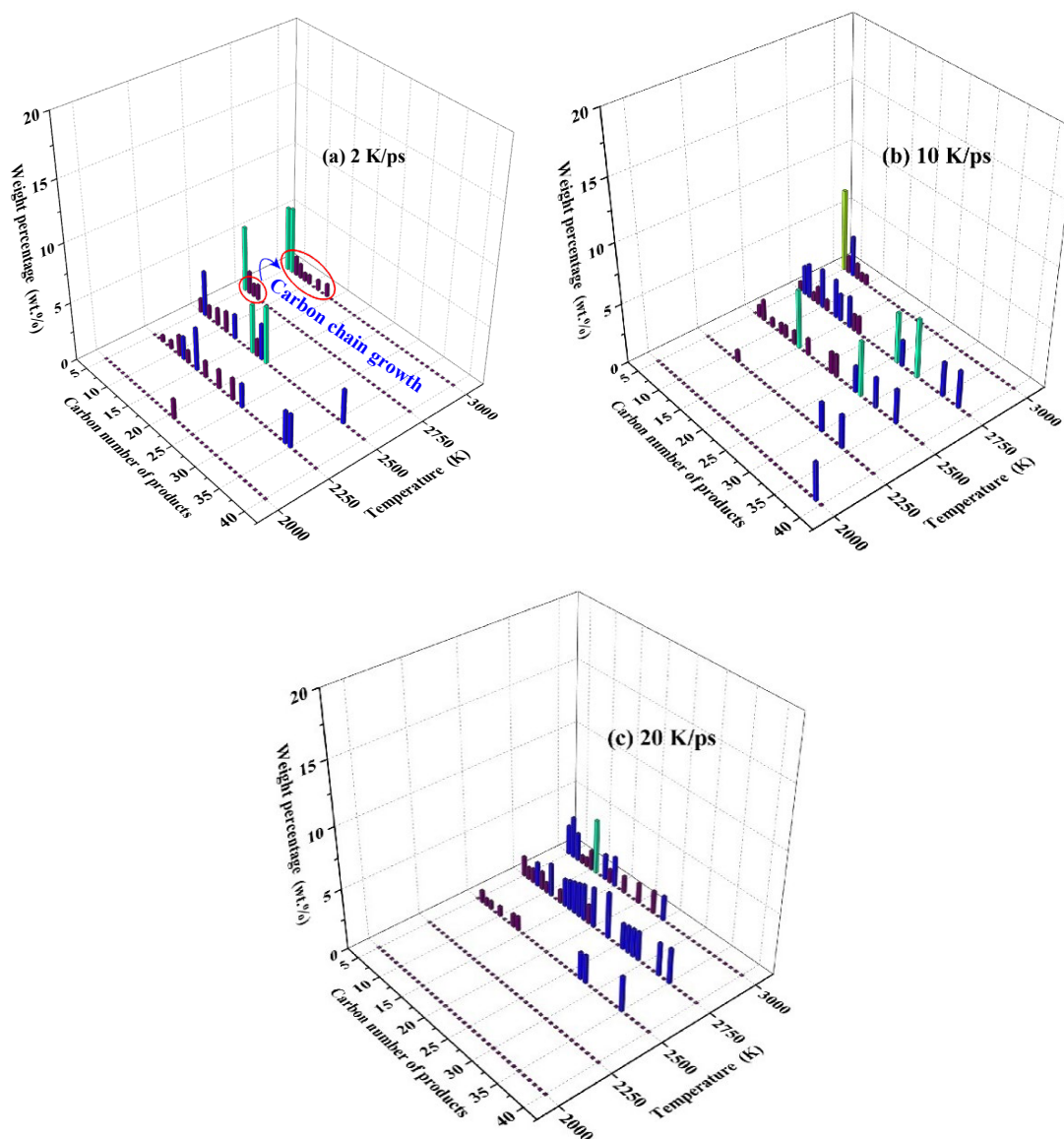

Fig. 4. Detailed distribution for products (C_5-C_{40}) during non-isothermal PE pyrolysis at typical temperatures: (a) 2 K/ps; (b) 10 K/ps and (c) 20 K/ps.

Statistical analyses of the specific gas products during PE pyrolysis suggest that the primary products are C_2H_4, C_3H_6, CH_4 and H_2. Normally, light olefins (C_2H_4 and C_3H_6) are important chemicals for PE pyrolysis recovery. Fig. 5 shows the evolution of these gases in 300-3000 K for PE pyrolysis at different heating rates. As shown in Fig. 5(a), more C_2H_4 is generated at lower temperatures at lower heating rates. Additionally, for the case of 2 K/ps, the molecular number of

C_2H_4 increases to the peak at around 2600 K and decreases with the further increase of temperature. However, there is no decrease stage of C_2H_4 for the cases of 10 K/ps and 20 K/ps. Similarly, as shown in Fig. 5(b), the evolutions of C_3H_6 under the three heating rates are similar to those for C_2H_4 in Fig. 5(a), except for lower molecule numbers. It can be seen that the peak yields of both C_2H_4 and C_3H_6 occur in the middle of the pyrolysis process at the heating rate of 2K/ps, while the corresponding maxima of the higher heating rates (10 K/ps and 20 K/ps) are both at the final temperature of 3000 K. Also, the peak yields of both C_2H_4 and C_3H_6 are higher at the lower heating rate. Fig. 5(c) and 5(d) indicate that there are also more H_2 and CH_4 generated at lower temperatures for lower heating rates. In addition, their molecular numbers keep increasing throughout the temperature range with higher rates of increase at higher temperatures. Finally, the reason for the molecular number decreasing of C_2H_4 and C_3H_6 at high temperature of 2600-3000K under 2 K/ps is supposed to be the addition reactions with radicals.
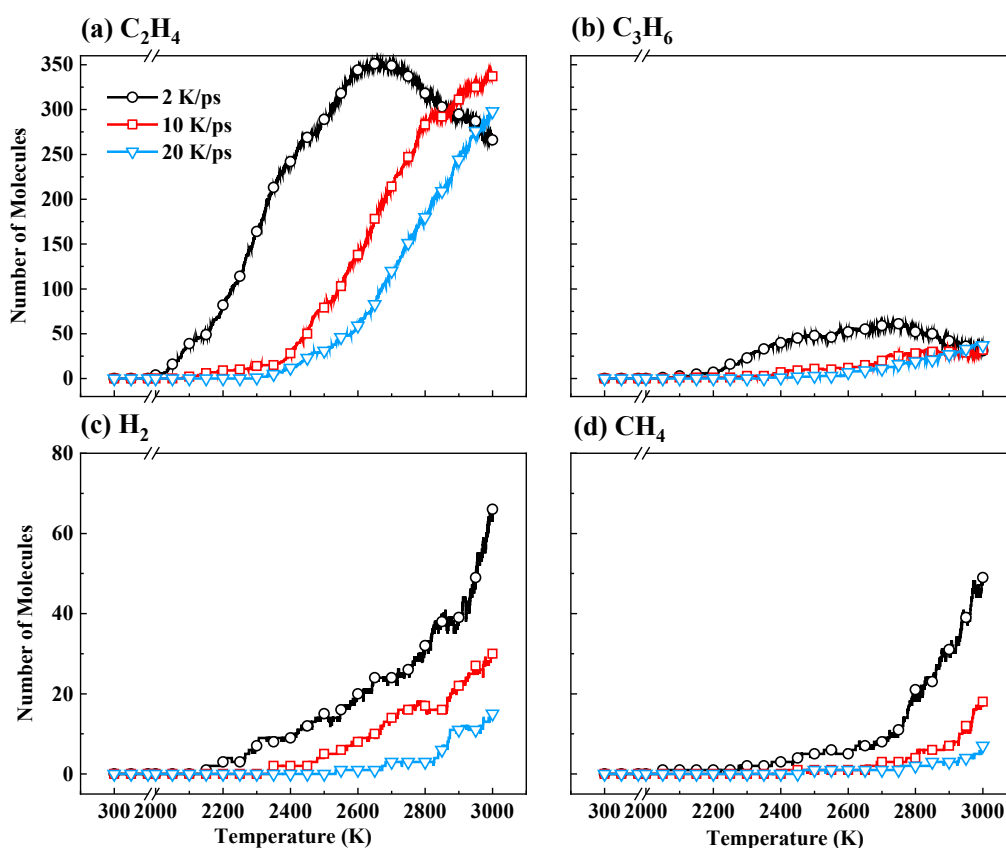

Fig. 5. Evolution of typical gas products in 300-3000 K for PE pyrolysis at different heating rates: (a) C_2H_4; (b) C_3H_6; (c) H_2 and (d) CH_4.

3.2. Isothermal pyrolysis of PE

The above analyses of the non-isothermal pyrolysis of PE suggest that the temperature and

reaction time play an important role in detailed compositions of the products, which was also illustrated in previous studies [37, 38]. Therefore, isothermal pyrolysis of PE is further conducted at typical high temperatures (2000, 2250, 2500, 2750, 3000, 3500 and 4000 K) for 250 ps. Fig. 6 shows the evolution of wax, oil and gas for PE pyrolysis at different temperatures, as well as the peak oil and the corresponding time. The results indicate that more oil is generated than gas in the early stages for all the isothermal pyrolysis conditions, which is different from the non-isothermal case of 2 K/ps. For the temperature as low as 2000 K, the gas and oil are slowly generated in 250 ps, as shown in Fig. 6(a). Much oil is generated rapidly in the early stage at higher temperatures and then further pyrolyzed into gas for the cases of 2500-3500 K. However, it is shown that the generated gas would decrease after reaching the peak value during the PE pyrolysis for those isothermal cases with constant temperatures higher than 2750 K. In Figs. 6(e)-(g), the trends are clearly shown for those with temperatures of 3000, 3500 and 4000 K. Finally, as shown in Figs. 6(f) and (g), the generated oil is about 30% in the later stage, which is clearly higher than that in Fig. 6(d). The results indicate that the generated gas might transformed into oil if the pyrolysis time is too long in high temperatures. As depicted in Fig. 6(h), the peaks of the oil are higher and appear earlier for the isothermal pyrolysis at higher temperatures.
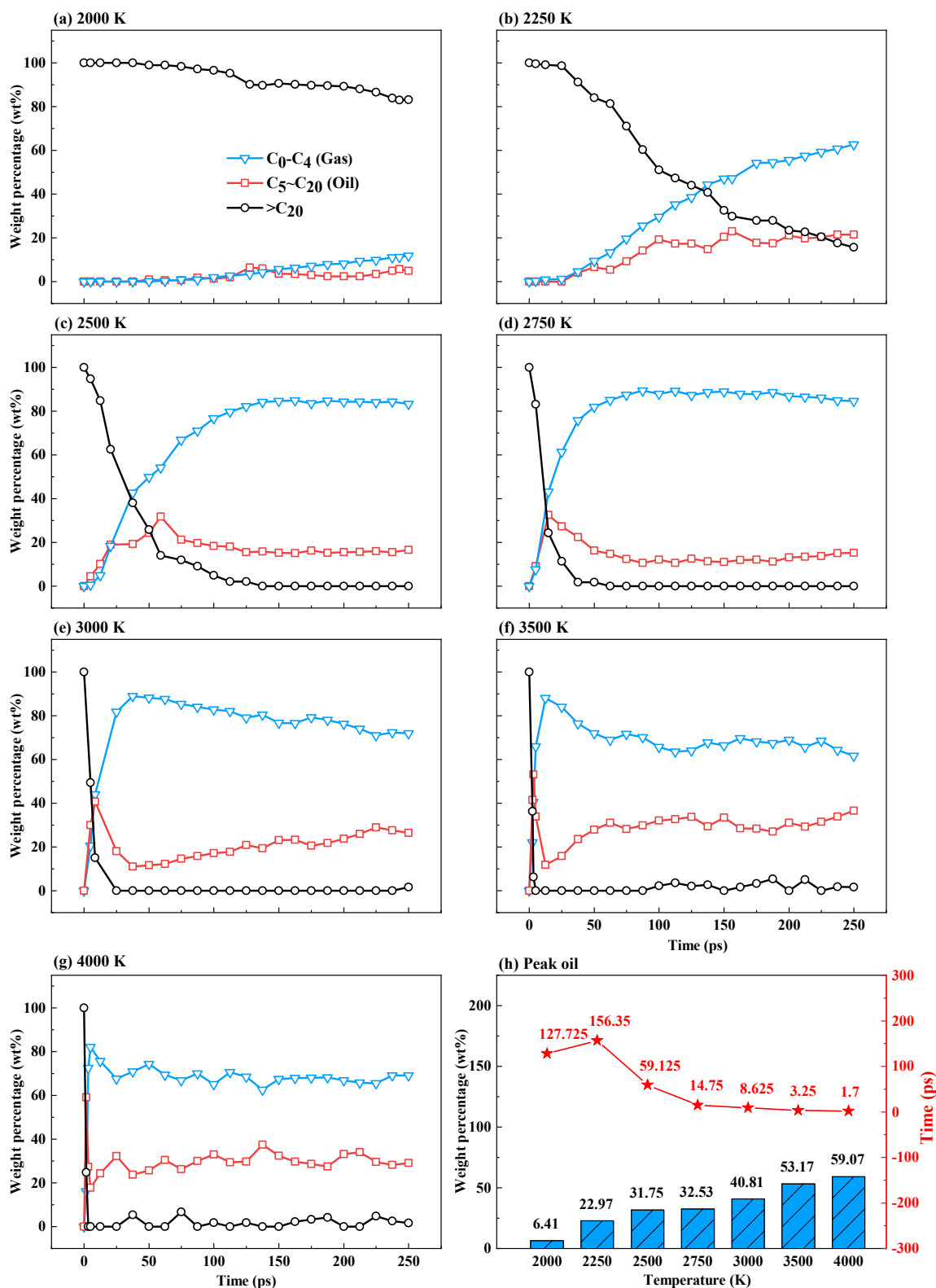
Fig. 6. Evolution of product groups (wax, oil and gas) for PE pyrolysis at different temperatures and the corresponding time for complete pyrolysis of char: (a) 2000 K; (b) 2250 K; (c) 2500 K; (d) 2750 K; (e) 3000 K; (f) 3500 K and (g) 4000 K; (h) Peak of oil and the corresponding time.
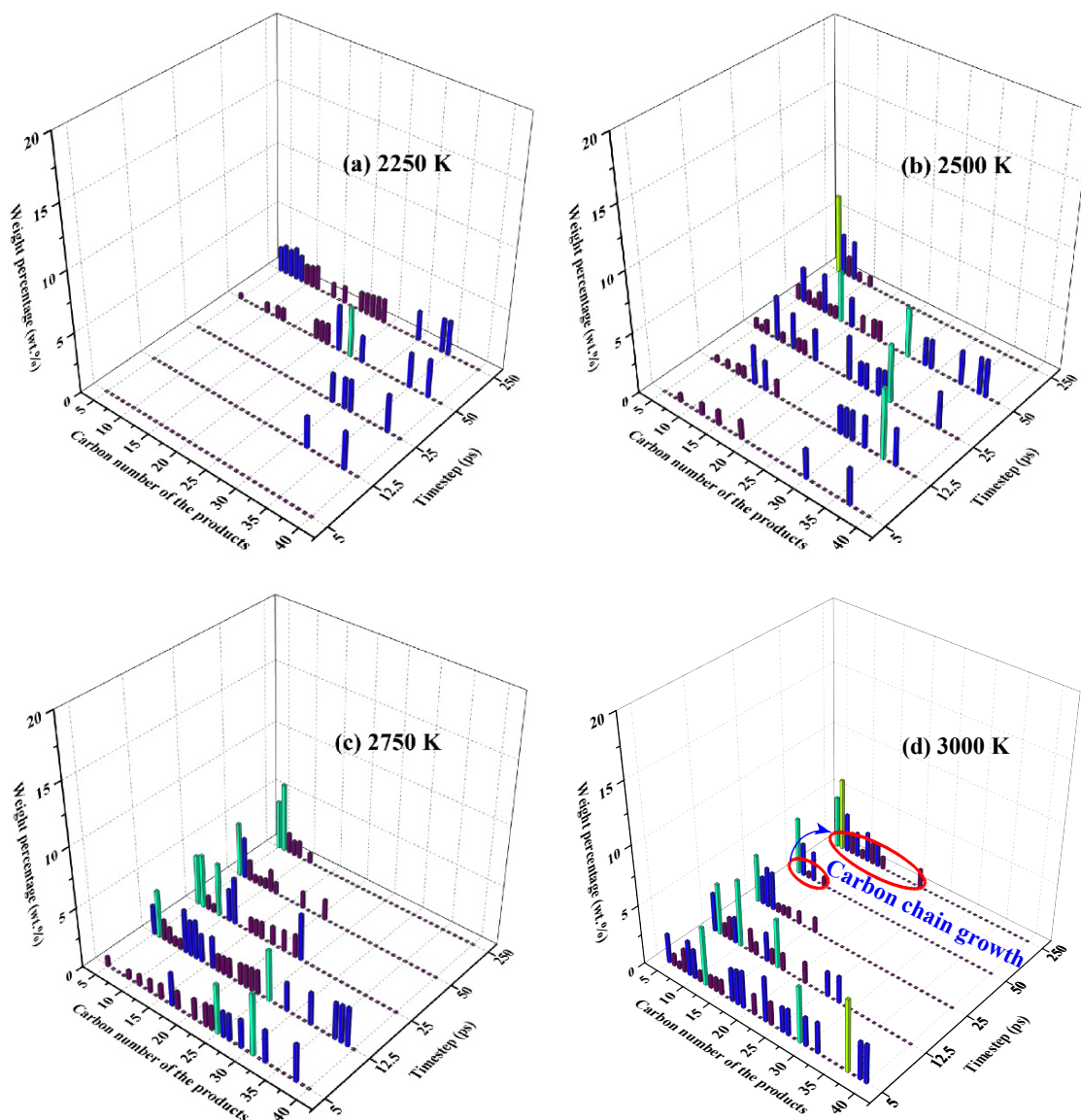
Fig. 7. Detailed distribution for products (C₅-C₄₀) during isothermal PE pyrolysis at typical time instants: (a) 2250 K; (b) 2500 K; (c) 2750 K and (d) 3000 K.

Fig. 7 shows the detailed distributions of C_5-C_{40} fractions at typical time instants during PE pyrolysis at temperatures of 2250, 2500, 2750 and 3000 K, respectively. The products with varied carbon numbers uniformly distributed can be generated under isothermal conditions with different temperatures, which is obviously different from those in Fig. 4 for non-isothermal cases. The corresponding pyrolysis time for the cases at higher temperatures is shorter. As shown in Fig. 7, the times are 250, 50, 12.5 and 5 ps fore pyrolysis temperatures of 2250, 2500, 2750 and 3000 K, respectively. Figs. 7(b)-(d) indicate that most of the long-chain components are further pyrolyzed into short-chain products in the later stage. In addition, as shown in Fig. 7(d), there are more products with longer chains at 250 ps than those at 50 ps, which suggests the growth of carbon chain in the later

stage at high temperatures again. For example, Fig. 7(d) illustrates that the weight percentage of C_6 products increases from 2.87% to 6.24% between 50 and 250 ps. As indicated in both Figs. 6 and 7, the critical temperature for the second increase of oil products is about 2750 K, which is similar to the results of non-isothermal pyrolysis at 2 K/ps.

Fig. 8 shows the evolution of the primary gases (C_2H_4, C_3H_6, CH_4 and H_2) during the isothermal PE pyrolysis at different temperatures for 250 ps. For C_2H_4, as shown in Fig. 8(c), the product molecular numbers decrease appreciably after reaching the peak for the cases with temperatures higher than 2750 K. Therefore, the final C_2H_4 generated in cases of 2750 to 4000 K is less than that at 2500 K, associated with the re-aggregation reactions in the later stage at high temperatures. The result is similar for the evolution of C_3H_6 generation, as shown in Fig. 8(a). It also indicates that the isothermal pyrolysis of PE at 2750 K is favorable for production of C_3H_6. Finally, as shown in Figs. 8 (b) and (d), more CH_4 and H_2 will be generated quickly at higher temperatures. For the PE pyrolysis at isothermal conditions, the generated CH_4 and H_2 are comparable with C_2H_4 and even more than C_3H_6, which is different from those at non-isothermal conditions. For the highest temperature of 4000 K, the obvious oscillation of the molecular number curves for the above four gases illustrates the strong reactions in the later stage of PE pyrolysis. Based on the above analyses, the isothermal pyrolysis of PE at 2500 or 2750 K is optimal for the generation of C_2H_4 and C_3H_6, which are the most important monomers recovered from PE waste.
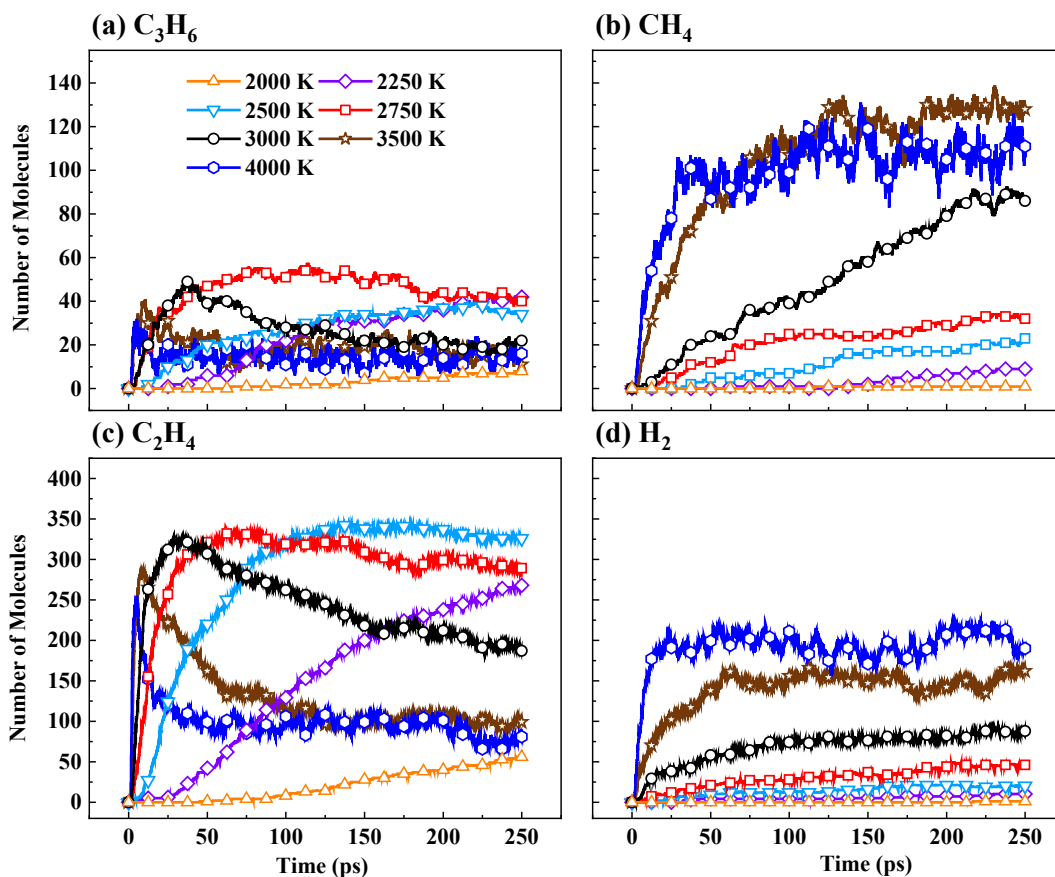
Fig. 8. Evolution of typical gas products in 250 ps for isothermal PE pyrolysis at different temperatures: (a) C_3H_6; (b) CH_4; (c) C_2H_4 and (d) H_2.

3.3. Comprehensive analysis of enhancing production of C_2H_4 and C_3H_6

In the above sub-sections, the evolution of PE pyrolysis products is analyzed separately for non-isothermal and isothermal conditions. Here the main parameters are further evaluated using light olefins (C_2H_4 and C_3H_6) as the target products, which are important for the recovery of fuels from PE waste. Fig. 9(a) shows a comprehensive comparison of the peak and final values of the C_2H_4 and C_3H_6 yield for various cases (both non-isothermal and isothermal conditions). It can be seen that at temperatures greater than 2500 K, the final yields of C_2H_4 and C_3H_6 are lower than the corresponding peak values due to the secondary reactions. The differences between the two values are greater for the isothermal cases with higher temperatures, especially at 3000, 3500 and 4000 K, which indicates the strong effect of reaction time. Temperature and reaction time are significant factors affecting the pyrolysis products in isothermal pyrolysis. Based on the results in Figs. 8(a) and (c), a decreasing trend was observed after reaching the peak yield with increasing reaction time in isothermal pyrolysis at comparatively high constant temperatures ($\geqslant$2500 K), due primarily to the secondary reactions of light olefins. In this study, the difference between the peak and final values is used to characterize the

16

negative effects of secondary reactions in continuous pyrolysis on the yield of light olefins. Specifically, the distributions of the peak C_2H_4 and C_3H_6 at different temperatures suggest that more C_2H_4 and C_3H_6 can be generated for the isothermal cases with temperatures in the range of 2500-3000 K. However, the obvious difference between the peak and final values at 3000 K indicates a significant adverse impact of the reaction time in the later stage of pyrolysis, especially for C_2H_4. Therefore, it can be concluded that 2500-2750 K is the optimal temperature range for isothermal pyrolysis for C_2H_4 and C_3H_6 recovery. Meanwhile, the temperatures for the peaks of C_2H_4 and C_3H_6 for non-isothermal pyrolysis with the heating rate of 2 K/ps are also in the range of 2500-2750 K. Previous works [21, 39] suggested that high temperature and short reaction time are helpful for obtaining high yields of light olefins. Fig. 9(b) illustrates the times corresponding to the peak yields of C_2H_4 and C_3H_6 at different temperatures ($\geq$2000 K) for isothermal pyrolysis. The effect of reaction time on light olefins depends on temperature. When the temperature is lower than 2500 K, the maximal production of C_2H_4 and C_3H_6 occurs at the end of pyrolysis. Once the temperature was increased to about 2500 K, the higher the temperature, the shorter the time corresponding to the peak yield. Overall, 2500-2750 K is the optimum temperature range for the recovery of light olefins by PE pyrolysis because of its high yield and mildly affected reaction time.
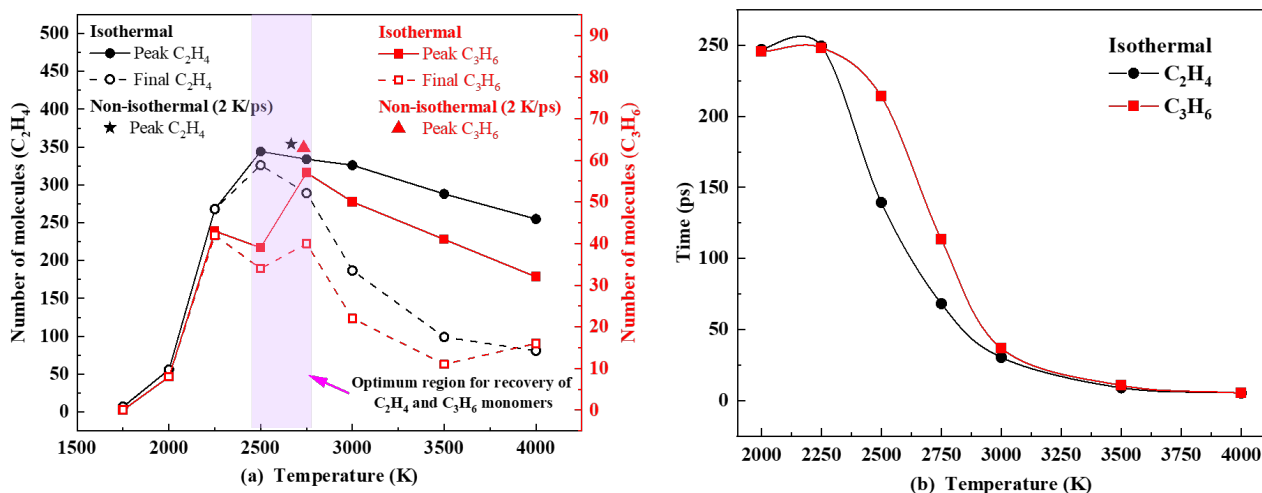

Fig. 9. (a) Comparison among the peak and final C_2H_4 and C_3H_6 products during the isothermal pyrolysis at different temperatures and non-isothermal one at 2 K/ps; (b) Corresponding times of peak yields of C_2H_4 and C_3H_6 under isothermal pyrolysis conditions.

3.4. Reaction pathways of C_2H_4 and C_3H_6

It is important to examine the mechanisms of C_2H_4 and C_3H_6 generation and consumption for the recovery of light olefins during PE pyrolysis. The detailed reactions during pyrolysis are identified and analyzed using the ReacNetGenerator software [40] based on the bond order information output

at 0.25 ps intervals during the simulations. Detailed information on the PE pyrolysis process and mechanisms are obtained for the cases at relatively low heating rates. The typical reactions for the generation and consumption of C_2H_4 and C_3H_6 are statistically analyzed at each stage. Fig. 10 shows the statistical analyses for the typical reactions of generation and consumption for C_2H_4 and C_3H_6 during PE non-isothermal pyrolysis at 2 K/ps. As shown in Figs. 10(a)-(c), β-fragmentation and its reverse radical addition are dominant elementary reactions related to C_2H_4. All reactions occur more frequently with the pyrolysis progress, mainly as a result of the temperature increase. Specifically, Fig. 10(b) indicates a decrease in reactions of β-fragmentation in Stage 3 compared to Stage 2, especially for C_2H_4. Combining Fig. 3(a), Fig. 5(a) and Fig. 10, it can be seen that β-fragmentation is more likely to occur in the long carbon chains ($>C_{20}$) than in the medium length carbon chains (C_5-C_{20}). Fig. 10(d) presents the typical reactions for the generation and consumption of C_2H_4 and C_3H_6, where some of them were also observed in previous studies [30, 41]. It should be noted that G-1~G-4 refer to the generation reaction pathways, while C-1~C-4 refer to the consumptions. The reactions of C_3H_6 are similar to those of C_2H_4, except that the H-abstraction is more significant. As illustrated in Fig. 10(c), more radical additions and H-abstraction reactions in Stage 4 lead to a decrease in the yield of C_2H_4 and C_3H_6, which are the main components of the gaseous products. These reactions are closely related to the free radicals, and the high temperature conditions in Stage 4 contributed to the large number of free radicals in the system. The consumption of C_2H_4 and C_3H_6 at high temperatures is mainly associated with their secondary reactions, where most of them are H-abstraction and radical addition reactions.
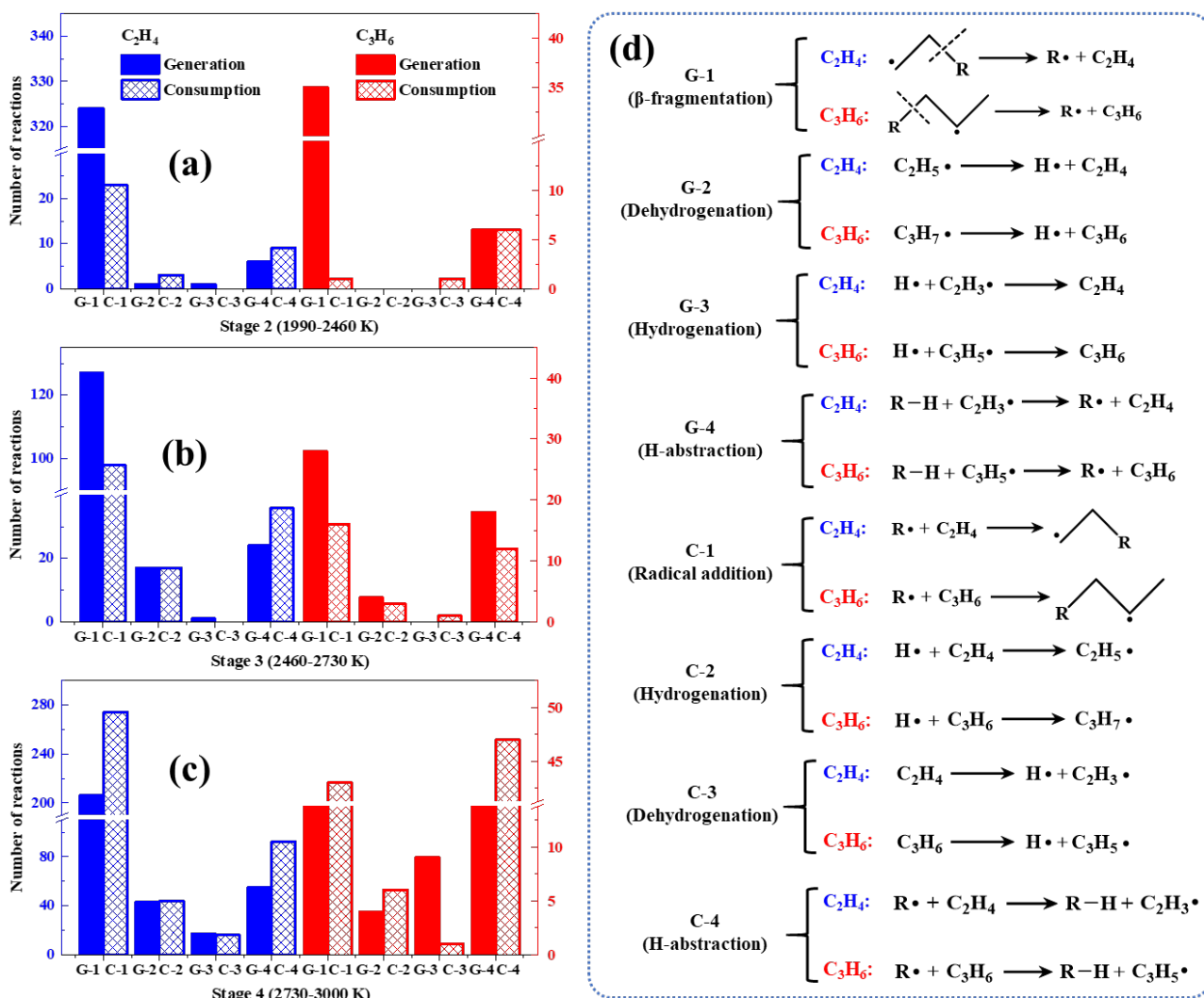
Fig. 10. Statistical analyses for the reactions of generation and consumption for C_2H_4 and C_3H_6 during PE non-isothermal pyrolysis at 2 K/ps: (a) Stage 2; (b) Stage 3; (c) Stage 4; and (d) Typical reactions for generation and consumption of C_2H_4 and C_3H_6.

The growth of carbon chains in the late stage at high temperature may be associated with the consumption of light olefins (C_2H_4 and C_3H_6). In the reaction process of PE pyrolysis, the growth of carbon chains due to free radical reactions mainly includes: (1) radical polymerization reaction with olefin monomers containing unsaturated double bonds [41] or (2) mutual coupling to form macromolecules [42]. Fig. 11 shows an example of the formation of long chain oil ($C_{10}H_{16}$) in Stage 4 during the non-isothermal pyrolysis at 2 K/ps. At 2953.5 K, $C_5H_7·$ and $C_3H_3·$ are produced by C_2H_4 through radical additions. Then, $C_5H_7·$ is transformed to $C_4H_5·$ at 2970 K after the processes of radical addition, H-abstraction, and β-fragmentation. Because of the easy breaking of the double bond of ethylene at high temperatures, ethylene radicals can be produced through free radical reactions. After that, at 2975 K, the ethylene radical is converted to $C_6H_{11}·$, which couples with $C_4H_5·$ and finally generates $C_{10}H_{16}$. Another example is the detailed production pathways for $C_{12}H_{12}$, as shown in Fig.

12. It indicates that through dehydrogenation, free radical reaction and H-transfer, ethylene is finally converted to $C_{10}H_{12}$ at 2965 K. Then, C_4H_6, C_3H_4 and $C_{10}H_9\cdot$ are generated through the β-fragmentation, H-abstraction and H-transfer of $C_{10}H_{12}$ and $C_7H_7\cdot$ at 2993.5 K. Finally, $C_{12}H_{12}$ is produced by the interactions among $C_{10}H_9$, C_3H_6 and H· at about 2998 K.
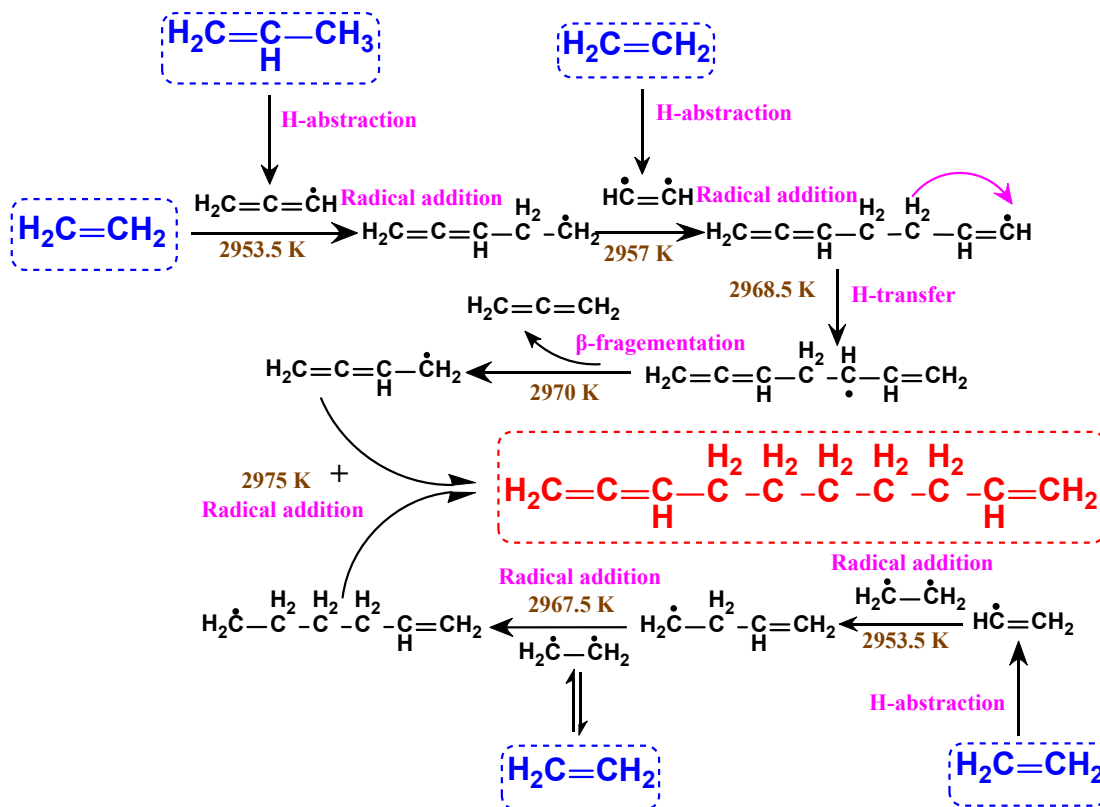

Fig. 11. An example of the detailed pathways for the formation of long-chain $C_{10}H_{16}$ through consuming C_2H_4 and C_3H_6 at the later stage of non-isothermal pyrolysis (2 K/ps).
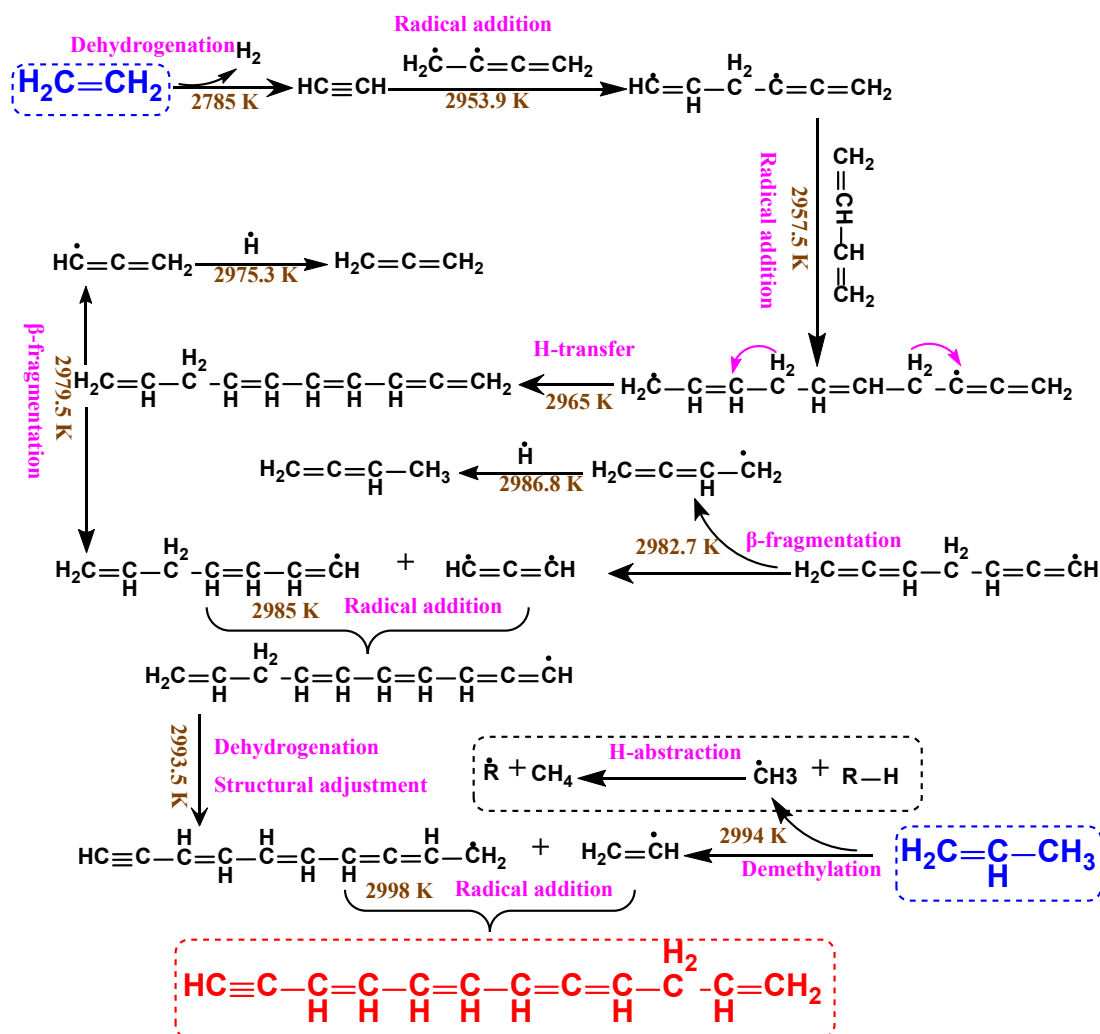
Fig. 12. An example of the detailed pathways for the formation of long-chain $C_{12}H_{12}$ through consuming C_2H_4 and C_3H_6 at the later stage of non-isothermal pyrolysis (2 K/ps).

The generation of relatively long-chain components in the late stage in isothermal pyrolysis at 3000 K is similar to the example pathways in Figs. 11 and 12. Fig. 13 shows an example of the detailed pathways for the formation of $C_{12}H_{12}$ and the consumption of C_2H_4 and C_3H_6. Over there, $C_3H_3\cdot$ and $C_3H_5\cdot$ are firstly generated through several dehydrogenation and H-abstraction reactions of C_3H_6. Then, at 216 ps, they are further synthesized into C_6H_8. After dehydrogenation, C_6H_8 is converted to $C_6H_6\cdot$. In this case, $C_{12}H_{12}$ is generated through the radical addition between two $C_6H_6\cdot$ at 248.75 ps. Another example of the formation of $C_{11}H_{15}\cdot$ is given in Fig. 14. At 244 ps, C_4H_8 is converted to $C_9H_{11}\cdot$ after several radical additions, demethylation and H-abstraction, etc. Finally, $C_{11}H_{15}\cdot$ is produced through the synthesizing of $C_9H_{11}\cdot$ and C_2H_4 at 245.68 ps.

Based on the above analyses of the detailed pathways of the consumption of C_2H_4 and C_3H_6, as well as the generation of long-chain compounds, it can be deduced that there are mainly two paths

leading to the decreasing of these olefin monomers in the later pyrolysis stage whether in non-isothermal (2 K/ps) or in isothermal ($\geq$2750 K) conditions. One is the H-abstraction reaction of C_2H_4 and C_3H_6 at high temperatures, in which compounds such as $C_2H_3\cdot$ and $C_3H_5\cdot$ etc. are generated. The other one is the activity increasing and the opening of carbon-carbon bonds of these monomers at high temperatures, which can be polymerized with radicals or each other. In this way, the polymerization of active monomers and radicals promotes the chain growth. On the whole, the secondary reactions (H-abstraction and radical addition) of C_2H_4 and C_3H_6 at high temperatures is the main reason for the decreasing of gas group and the increasing of oil as shown in the final stage in Fig. 3(a) and Figs. 6(d) - (g).
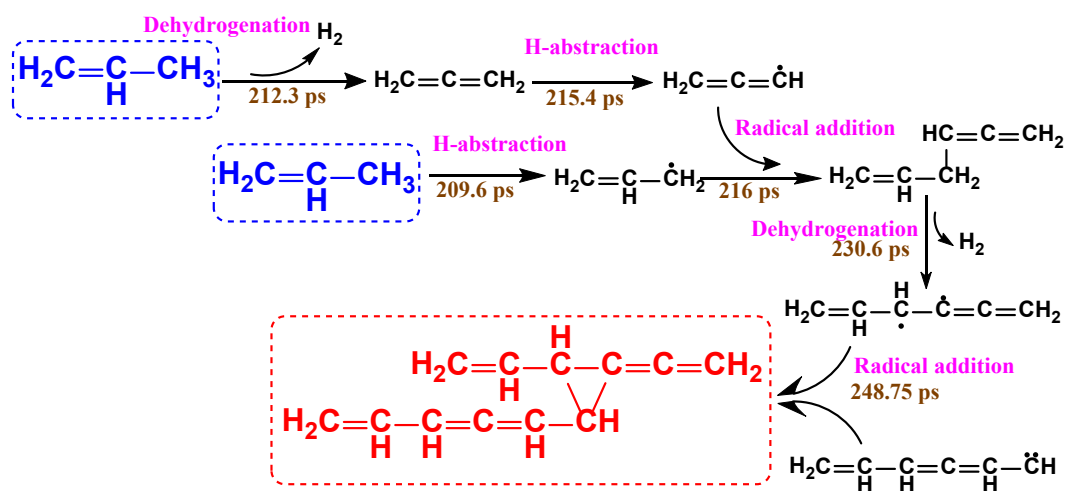
Fig. 13. An example of the detailed pathways for the formation of long-chain $C_{12}H_{12}$ through consuming C_2H_4 and C_3H_6 at the later stage of isothermal pyrolysis (3000 K).
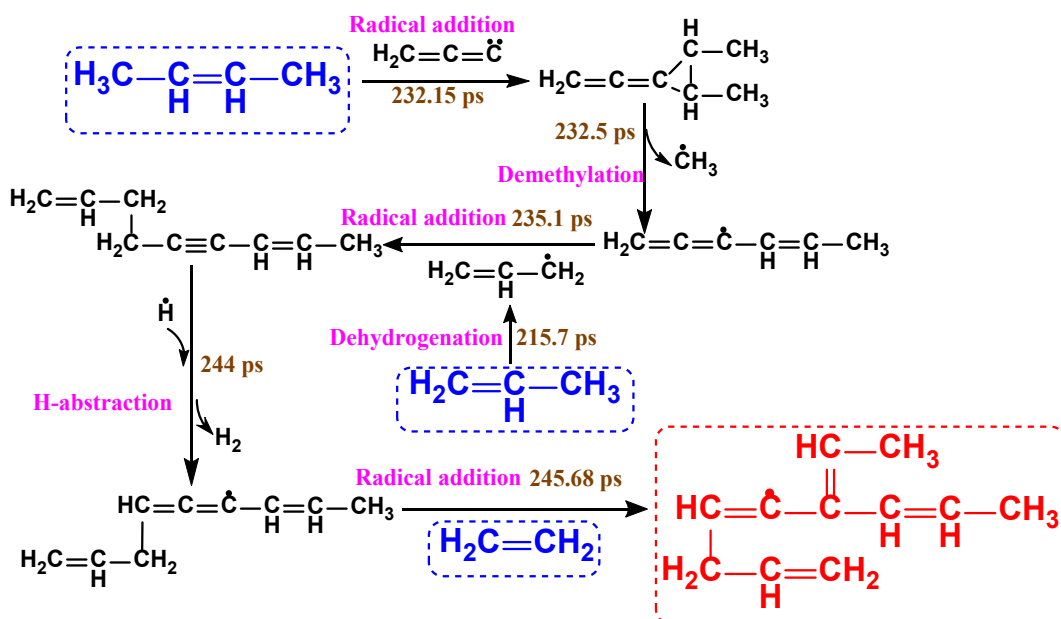
Fig. 14. An example of the detailed pathways for the formation of long-chain $C_{11}H_{15}\cdot$ through consuming

C_2H_4 and C_3H_6 at the later stage of isothermal pyrolysis (3000 K).

4. Concluding remarks

This study is focused on understanding the process and chemical reactions in PE pyrolysis, in order to achieve optimal chemicals and fuels recovery from plastic wastes. The detailed pyrolysis process and product distribution are studied for PE waste using ReaxFF MD simulation for both non-isothermal and isothermal conditions. The major conclusions are:

(1) The PE pyrolysis at non-isothermal conditions can be divided into four stages. The last stage (post pyrolysis) is analyzed in depth, which shows decreasing of short-chain products and increasing of relatively long-chain components at high temperatures.

(2) The heating rate plays an important role in both the evolution of gas and oil and the detailed distribution of products with different carbon numbers during the PE non-isothermal pyrolysis. Pyrolysis at higher heating rate reduces the cracking of the oil and leads to a higher oil yield, and promotes the C_5-C_{40} products with a uniform carbon number distribution.

(3) The PE pyrolysis at isothermal conditions shows that much oil is generated rapidly in the early stage at higher temperatures and then further pyrolyzed into gas for the cases of 2500-3500 K. Additionally, the amount of gas products would decrease after reaching the peak for the case with temperatures higher than 2750 K, which is caused by the secondary reactions of olefins.

(4) The effect of reaction time on yields of light olefins depends on pyrolysis temperatures. Under isothermal pyrolysis conditions, 2500-2750 K is the best pyrolysis temperature range for PE pyrolysis recovery C_2H_4 and C_3H_6 due to its high yield and mild negative effect of reaction time.

(5) Finally, detailed generation and consumption pathways of C_2H_4 and C_3H_6 and generation of long-chain fractions of PE pyrolysis are investigated. The statistics of the main reactions of ethylene production and consumption in non-isothermal pyrolysis at 2 K/ps are analyzed. The results suggest that H-abstraction and radical additions are the main reactions for the yield decrease in the later stages of pyrolysis. The reaction pathways illustrate the mechanisms of the transformation of C_2H_4 and C_3H_6 into long carbon chain molecules at high temperatures for both non-isothermal and isothermal conditions.

The molecular understanding of the process and chemical reactions in PE pyrolysis obtained by the MD simulation provides useful insight into the combined effects and the relationships of various parameters of the pyrolysis. In order to achieve optimal chemicals and fuels recovery from plastic wastes in practical applications, a complete mapping of the parameters between the conditions used

in MD simulation and experimental study of pyrolysis needs to be further investigated.

Acknowledgement

References

[1] Al-Salem SM, Lettieri P, Baeyens J. Recycling and recovery routes of plastic solid waste (PSW): A review. Waste Manage. 2009;29:2625-43.

[2] Ragaert K, Delva L, Van Geem K. Mechanical and chemical recycling of solid plastic waste. Waste Manage. 2017;69:24-58.

[3] Vollmer I, Jenks MJF, Roelands MCP, White RJ, van Harmelen T, de Wild P, et al. Beyond Mechanical Recycling: Giving New Life to Plastic Waste. Angew Chem Int Edit. 2020;59:15402-23.

[4] Li CT, Zhuang HK, Hsieh LT, Lee WJ, Tsao MC. PAH emission from the incineration of three plastic wastes. Environ Int. 2001;27:61-7.

[5] Lopez G, Artetxe M, Amutio M, Alvarez J, Bilbao J, Olazar M. Recent advances in the gasification of waste plastics. A critical overview. Renew Sust Energ Rev. 2018;82:576-96.

[6] Solis M, Silveira S. Technologies for chemical recycling of household plastics - A technical review and TRL assessment. Waste Manage. 2020;105:128-38.

[7] Wong SL, Ngadi N, Abdullah TAT, Inuwa IM. Current state and future prospects of plastic waste as source of fuel: A review. Renew Sust Energ Rev. 2015;50:1167-80.

[8] Kaminsky W, Predel M, Sadiki A. Feedstock recycling of polymers by pyrolysis in a fluidised bed. Polym Degrad Stabil. 2004;85:1045-50.

[9] Sharuddin SDA, Abnisa F, Daud WMAW, Aroua MK. A review on pyrolysis of plastic wastes. Energ Convers Manage. 2016;115:308-26.

[10] Aguado J, Serrano DP, Escola JM. Fuels from Waste Plastics by Thermal and Catalytic Processes: A Review. Ind Eng Chem Res. 2008;47:7982-92.

[11] Al-Salem SM. Thermal pyrolysis of high density polyethylene (HDPE) in a novel fixed bed reactor system for the production of high value gasoline range hydrocarbons (HC). Process Saf Environ. 2019;127:171-9.

[12] Pan RM, Martins MF, Debenest G. Pyrolysis of waste polyethylene in a semi-batch reactor to produce liquid fuel: Optimization of operating conditions. Energ Convers Manage. 2021;237.

[13] Onwudili JA, Insura N, Williams PT. Composition of products from the pyrolysis of polyethylene and polystyrene in a closed batch reactor: Effects of temperature and residence time. J Anal Appl Pyrol. 2009;86:293-303.

[14] Mastral FJ, Esperanza E, Garcia P, Juste M. Pyrolysis of high-density polyethylene in a fluidised bed reactor. Influence of the temperature and residence time. J Anal Appl Pyrol. 2002;63:1-15.

[15] Sodero SF, Berruti F, Behie LA. Ultrapyrolytic cracking of polyethylene - A high yield recycling method. Chem Eng Sci. 1996;51:2805-10.

[16] Marcilla A, Beltran MI, Navarro R. Thermal and catalytic pyrolysis of polyethylene over HZSM5 and HUSY zeolites in a batch reactor under dynamic conditions. Appl Catal B-Environ. 2009;86:78-86.

[17] Elordi G, Olazar M, Lopez G, Amutio M, Artetxe M, Aguado R, et al. Catalytic pyrolysis of HDPE in continuous mode over zeolite catalysts in a conical spouted bed reactor. J Anal Appl Pyrol. 2009;85:345-51.

[18] Elordi G, Olazar M, Lopez G, Artetxe M, Bilbao J. Product Yields and Compositions in the Continuous Pyrolysis of High-Density Polyethylene in a Conical Spouted Bed Reactor. Ind Eng Chem Res. 2011;50:6650-9.

[19] Williams PT, Slaney E. Analysis of products from the pyrolysis and liquefaction of single plastics and waste plastic mixtures. Resour Conserv Recy. 2007;51:754-69.

[20] Hernandez MD, Garcia AN, Marcilla A. Study of the gases obtained in thermal and catalytic flash pyrolysis of HDPE in a fluidized bed reactor. J Anal Appl Pyrol. 2005;73:314-22.

[21] Conesa JA, Font R, Marcilla A, Garcia AN. Pyrolysis of Polyethylene in a Fluidized-Bed Reactor. Energ Fuel. 1994;8:1238-46.

[22] Zhang YQ, He HY, Liu YR, Wang YL, Huo F, Fan MH, et al. Recent progress in theoretical and computational studies on the utilization of lignocellulosic materials. Green Chem. 2019;21:9-35.

[23] Feng T, Li MM, Zhou JJ, Zhuang HN, Chen F, Ye R, et al. Application of molecular dynamics simulation in food carbohydrate research-a review. Innov Food Sci Emerg. 2015;31:1-13.

[24] van Duin ACT, Dasgupta S, Lorant F, Goddard WA. ReaxFF: A reactive force field for hydrocarbons. J Phys Chem A. 2001;105:9396-409.

[25] Hong D, Si T, Guo X. Insight into the calcium carboxylate release behavior during Zhundong coal pyrolysis and combustion. Proceedings of the Combustion Institute. 2021;38:4023-32.

[26] Hong DK, Li P, Si T, Guo X. ReaxFF simulations of the synergistic effect mechanisms during co-pyrolysis of coal and polyethylene/polystyrene. Energy. 2021;218.

[27] Batuer A, Chen D, He X, Huang Z. Simulation methods of cotton pyrolysis based on ReaxFF and the influence of volatile removal ratio on volatile evolution and char formation. Chemical Engineering Journal. 2021;405:126633.

[28] Chen C, Volpe R, Jiang X. A molecular investigation on lignin thermochemical conversion and carbonaceous organics deposition induced catalyst deactivation. Applied Energy. 2021;302:117557.

[29] Hong DK, Gao P, Wang CB. A comprehensive understanding of the synergistic effect during co-pyrolysis of polyvinyl chloride (PVC) and coal. Energy. 2022;239.

[30] Liu XL, Li XX, Liu J, Wang Z, Kong B, Gong XM, et al. Study of high density polyethylene (HDPE) pyrolysis with reactive molecular dynamics. Polym Degrad Stabil. 2014;104:62-70.

[31] Wang YZ, Li YJ, Zhang CX, Yang LG, Fan XX, Chu LZ. A study on co-pyrolysis mechanisms of biomass and polyethylene via ReaxFF molecular dynamic simulation and density functional theory. Process Saf Environ. 2021;150:22-35.

[32] Sorensen MR, Voter AF. Temperature-accelerated dynamics for simulation of infrequent events. J Chem Phys. 2000;112:9599-606.

[33] Yan S, Xia DH, Liu XJ. Beneficial migration of sulfur element during scrap tire depolymerization with supercritical water: A molecular dynamics and DFT study. Sci Total Environ. 2021;776.

[34] Hong DK, Si T, Guo X. Insight into the calcium carboxylate release behavior during Zhundong coal pyrolysis and combustion. P Combust Inst. 2021;38:4023-32.

[35] Large-scale Atomic/molecular massively Parallel simulator (LAMMPS), Sandia National Labs.

[36] Chenoweth K, van Duin ACT, Goddard WA. ReaxFF reactive force field for molecular dynamics simulations of hydrocarbon oxidation. J Phys Chem A. 2008;112:1040-53.

[37] Lopez G, Artetxe M, Amutio M, Bilbao J, Olazar M. Thermochemical routes for the valorization of waste polyolefinic plastics to produce fuels and chemicals. A review. Renew Sust Energ Rev. 2017;73:346-68.

[38] Zhao DT, Wang XH, Miller JB, Huber GW. The Chemistry and Kinetics of Polyethylene

Pyrolysis: A Process to Produce Fuels and Chemicals. Chemsuschem. 2020;13:1764-74.

[39] Milne BJ, Behie LA, Berruti F. Recycling of waste plastics by ultrapyrolysis using an internally circulating fluidized bed reactor. J Anal Appl Pyrol. 1999;51:157-66.

[40] Zeng JZ, Cao LQ, Chin CH, Ren HS, Zhang JZH, Zhu T. ReacNetGenerator: an automatic reaction network generator for reactive molecular dynamics simulations. Phys Chem Chem Phys. 2020;22:683-91.

[41] Vinu R, Broadbelt LJ. Unraveling Reaction Pathways and Specifying Reaction Kinetics for Complex Systems. Annu Rev Chem Biomol. 2012;3:29-54.

[42] Ranzi E, Dente M, Goldaniga A, Bozzano G, Faravelli T. Lumping procedures in detailed kinetic modeling of gasification, pyrolysis, partial oxidation and combustion of hydrocarbon mixtures. Prog Energ Combust. 2001;27:99-139.